Probable Cracking Development in Axial Dovetail Joints of Aero Engine Compressor Discs

M. M. I. Hammouda[1], R. A. Pasha[1] and I. G. El-Batanony[2]

[1] MED, University of Engineering and Technology (UET), Taxila, Pakistan
[2] MED, Al Azhar University, Cairo, Egypt

ABSTRACT. *This paper presents a numerically-based methodology for the prediction of probable sites of fretting fatigue cracks initiated at the common surfaces of axial dovetail joints of an aero-engine compressor. The entrance angles of the initiated cracks and the possibility of their development are modeled. Further, the paper suggests a possible surface cracking mechanism for the formation of free relatively large material particles found by other researchers filling the mouth of cracks initiated by fretting fatigue. The proposals result from an incremental two-dimensional elastic-plastic finite element simulation of two loading cycles applied to a sector representing the disc-blades assembly in a typical compressor. One cycle includes disc acceleration, full blade loading and unloading and final deceleration. The analysis assumes that (1) the fretted surfaces are frictional with a coefficient of 0.25 and (2) cracks likely initiate in regions of cyclic plasticity along the plane of maximum shear stress range and develop in regions of tension. The generated stress strain field is multi axial and non-proportional. Thus, the present analysis searches for relevant critical planes. The present results show that (1) multiple cracking with different orientation are probable in the fretted material nearest to the joint notch base (2) initiated cracks can have cyclic tensile stress ranges sufficient for their stage II mode I growth and (3) initiated cracks can become dormant due to the existence of local compressive stress field.*

INTRODUCTION

Fretting fatigue (FF) is often responsible for the damage at attachments of structural components. This type of damage is very complex as it involves surface and subsurface multi axial non-proportional elastic-plastic cyclic stress-strain fields [1], early crack nucleation [2] at multiple contact sites [3] and wear by the formation of debris and small particles due to microscopic fatigue of surface asperities, e.g. [1, 2] and oxidation of the contact surfaces. Thus, roughness of the fretted surfaces, their friction coefficient and the tribological system drastically change. The existence of debris and small particles [1] either in contact with the two mating surfaces or as a shield in the mouth or between the flanks of nucleated surface cracks further complicates the problem.

The events possibly taking place during FF follow. Irreversible flow at the surface and within depths of only several grains leads to intrusions, extrusions and finally to cracks [1, 4]. Local cyclic plastic shear deformation controls the process of FCI [5]. Multiple crack initiation sites [4, 5] with different angles are common. This can be a result of local micro structural differences and the generated non-proportional stress field. The early life of the initiated cracks is consumed in stage I growth [4]. Retardation in growth of some of those cracks is most likely due to sharply decreasing stress fields [6], tri-axial compressive stresses

associated with friction between crack flanks and residual compressive stresses within the fretted material [7]. Thus, numerous of the initiated cracks stop propagation [1]. Experimental evidences [1, 4] show the existence of relatively large broken material particles filling the mouth of cracks. One or two cracks may be able to dominate and propagate to cause failure.

Numerical manipulation of FF was mostly within the context of experimental setup designed to simplify real applications. Each application has its mechanical behavior and requires a separate manipulation. An application of particular importance is the blade-disk dovetail attachments in aero-engines. Fretting FCI life is crucial in those attachments. Numerical and experimental studies simulated loaded disc-blades assembly, e.g. [10, 11]. Used loads do not match loading during the normal engine cycle [12]. This work numerically manipulates axial dovetail fixings in typical operations and predicts probable sites of fretting FCI, the entrance angles of the initiated cracks and their development possibility. The results suggest a surface cracking mechanism for the formation of free relatively large material particles possibly found filling the mouth of FF cracks. The tool is a two-dimensional elastic-plastic finite element (FE) modeling.

PRESENT WORK

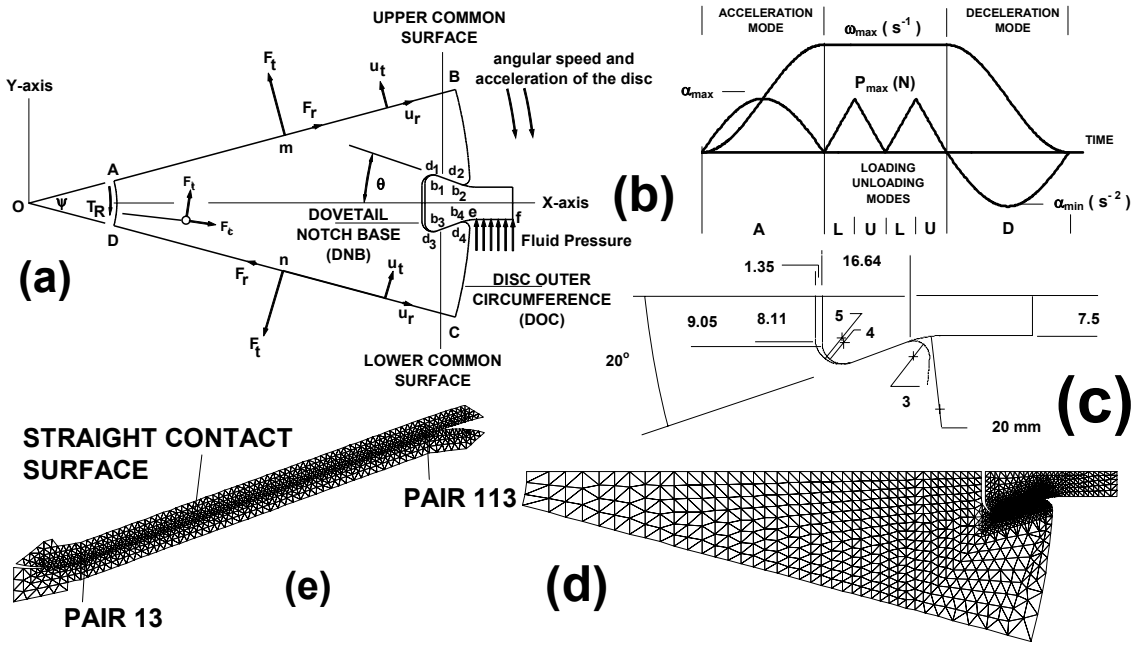

Fig. 1 Present application (a) a single sector with its boundary conditions, (b) modes simulating loading conditions during a cycle (c) dimensions of the analysed dovetail joint, (d) half of the analysed mesh and (e) magnification of the model lower half

A disc-blades assembly of an aero-engine compressor is assumed mounted on a circular rotor. The blades are assembled into the disc with Coulomb frictional dovetail joints. The disc is divided into identical sectors. The sector shown in Fig. 1(a) is analysed with inertia forces distributed over the body. The sector is externally subject to forces acting at its border

surfaces with its surrounding. Appropriate boundary conditions are devised to preserve the disc continuity. Elastic-plastic FE package [13] is utilised. The von-Mises yield criterion and the Prandtl-Reuss flow rule with kinematics hardening are adopted. In the plastic regime, a simple power stress-strain law is assumed.

After the application of the boundary conditions, a system of algebraic equations is generated. The present solution adopts a previously published mathematical treatment [13] purposely devised to manipulate the stiffness matrix with no need of iteration. The analysis starts with the disc appropriately supported, initially un-deformed and having all the contact pairs along the straight common surfaces assumed sticking. The schematic of Fig. 1(b) shows a loading cycle. The first increment of the acceleration mode is marched to have the corresponding incremental inertia forces applied.

The problem is solved for the displacement field and the internal forces acting along the common surfaces. The relevant kinematics and kinetic data given by the resulting solution are used to update the contact regime of each pair. The new contact data are induced to the boundary conditions of the problem to compute a new solution. Such an iterative procedure is terminated when the resulting contact regimes do not violate any of the basic contact concepts. A new time increment is successively allowed until the maximum disc speed is reached. During the acceleration and deceleration modes the variation of the disc angular speed and acceleration with time are assumed sinusoidal. Similarly, the blade is incrementally loaded until maximum pressure is achieved. Incremental unloading, then, loading and unloading follows. The disc is, then, incrementally decelerated until it stops. Further cycles can, then, be applied.

During an increment step, possible events are recognised as (1) the change in contact regimes, (2) the change in elastic-plastic regimes and (3) the achievement of the next maximum or zero value of the loading modes. The candidates corresponding to each event are identified. A minimum factor is computed for the occurrence of an event within its candidates. Such minimum values recognise which event is to take place and the corresponding factor which decides the current increment. Thus, all the initial parameters necessary as inputs for the next step are computed. Consequently, deformation, internal force and stress-strain fields are continuously traced.

Figure 1(c) shows the geometries [3] used in this work. The geometry corresponds to the compressor of the Jumbo jets engine RB211. Figures 1(d, e) show the corresponding mesh. Each disc/blade common surface had 125 equally spaced contact pairs. The plane strain analysis was assumed. The present results correspond to a friction coefficient of 0.25. The system was analysed for a maximum disc speed of 12000 rpm, a full blade load of 1000 N and an acceleration/deceleration time of 6 minutes. Two cycles were simulated. The material of the assembly was Ti-6Al-4V [3]. The elasticity modulus, the Poisson's ratio, the strain hardening exponent and the density were respectively 114 GPa, 0.33, 0.2 and 4429 kg/m^3. The yield stress of that alloy ranges between 930 and 1100 MPa. Its endurance limit was found [14] between 350 MPa and 380 MPa. Since non-propagating initiated surface cracks can exist below the fatigue limit of smooth specimens, the present analysis used a value of 350 MPa as a rough estimate of the yield stress.

RESULTS AND DISCUSSION

This work tackles the problems of the numerical analysis of a realistic loading, the interface frictional behaviour, the plasticity induced and the possible fretting FCI and their

development. The mechanical behaviour of the contact pairs along the joint common surfaces were traced to continuously check that the basic macro mechanics of contact was not violated anywhere. This included the development of the relative tangential and normal displacements along the common surfaces and the corresponding contact forces and regimes. The contact pairs on both common surfaces cyclically slip. For most of the pairs, the application of a loading cycle results in outward and inward sliding of the blade relative to the disc. Entire outward sliding starts on accelerating the disc. That sliding is terminated at the end of the acceleration mode for the upper common surface (UCS) and at the end of the next loading mode for the lower common surface (LCS). Inward sliding is a result of decelerating the disc. Generally, the LCS experiences more range of cyclic slipping than the UCS. The inertia forces due to the tangential acceleration are responsible for that difference. Figure 2 presents the work done by the friction force. This shear-slip work may be utilised as a damage parameter [12]. Thus, both common surfaces are susceptible to damage and pair 13 on the LCS is expected to be the most susceptible site to damage.

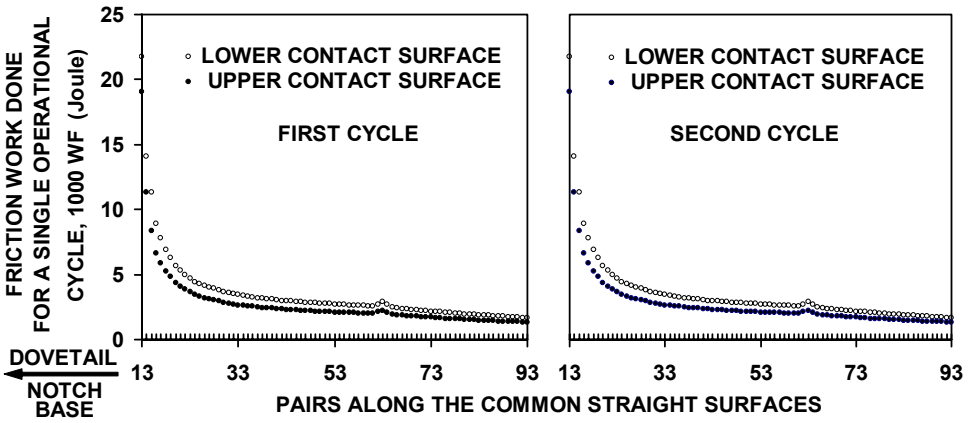

Fig. 2 Work done by the tangential friction force during both simulated cycles for each pair along the two common surfaces in the course of two operational cycles

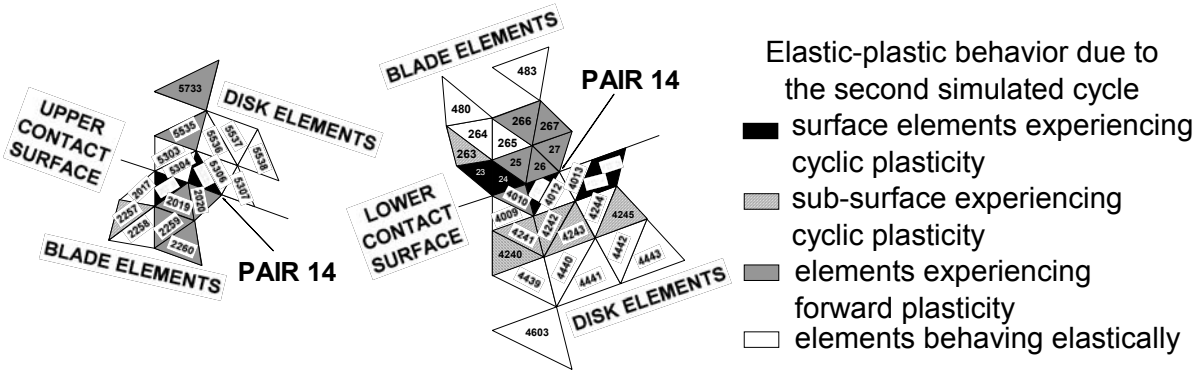

Fig. 3 all elements, which experience plastic strain during two simulated cycles

Invariably, plasticity is developed neighbouring to the edges of the joint nearest to the dovetail notch base (DNB), on the disk and the blade sides along the LCS, and UCS. At

some stages, plasticity extends deeper through the material of both parts of the joint. Fatigue cracks are likely to initiate at the surface in regions of cyclic plasticity [1, 4]. This concept is applied to predict probable sites of fretting FCI. Figure 3 shows the 49 disk and blade elements which experience plastic deformation during two simulated cycles. The behaviour of the elements as a result of the second load cycle was considered representative if load cycles are further repeated. Fourteen elements experience cyclic plastic deformation. Out of those elements four disc elements and three blade elements have boundaries on the common surfaces, shown black in Fig. 3. Those elements are probable sites of FCI. The present analysis indicates the possibility of having multiple FCI sites along the contact surfaces near the DNB.

For modeling, the present work used the assumption of single yield strength. This means that the present work assumes that strain localization in the relevant elements governs the crack initiation sites. The analysis assumed homogeneous and isotropic titanium alloy and did not consider the effect of the material microstructure features on the crack initiation sites. However, FF is widely considered a high cycle fatigue phenomenon, which can occur in the absence of macroscopic plasticity although micro-plasticity is involved. Under low cycling remote stresses far beyond the macroscopic yield strength of the material, plastic slip occurs in a few surface grains, and cracks eventually nucleate. This takes place in well-orientated relatively large grains such that their slip planes are subject to the largest resolved shear stress. Other grains remain elastic. Thus, surface yield stress is significantly less than the bulk yield stress. Furthermore, the surface yield stress is sensitive to the surfaces roughness. Thus, the yield stress used in the present analysis, i.e. 350 MPa, was lower than macroscopic yield stress of the material, i.e. approximately 1000 MPa, and close to its endurance limit, i.e. approximately 360 MPa. Obviously, due to the various micro-structural features distributed on the surface, surface yield stress can also locally vary and, as a result, different sites on the surface behave uniquely. Other factors can affect the multiplicity of FCI sites such as (i) variation in the speed of the disc, (ii) change in fluid pressure and (iii) blade vibration.

Table 1 $\Delta\tau_{max}$, $\Delta\sigma_{Tmax}$ and $\Delta\sigma_{max}$ acting on the probable initiation sites and their corresponding plane angles, $\alpha^{\setminus}$, $\alpha^{\setminus\setminus}$ and $\alpha^{\setminus\setminus\setminus}$; $\Delta\gamma^{p}_{max,}$ $\Delta\gamma^{p}_{c}$ and $\Delta\gamma^{p}_{r}$ are the maximum cyclic plastic shear strain range and its reversed cyclic and ratcheting components.

Elements having cyclic plastic strains	Plane of Maximum Shear Stress Range							Plane of Maximum tensile Stress Range				Stress Range			
	$\alpha^{\setminus}$	τ_{min}	τ_{max}	$\Delta\tau$	$\Delta\gamma^{p}_{c}$	$\Delta\gamma^{p}_{r}$	$\Delta\gamma^{p}_{max}$	$\alpha^{\setminus\setminus}$	σ_{min}	σ_{max}	$\Delta\sigma_{T}$	$\alpha^{\setminus\setminus\setminus}$	σ_{min}	σ_{max}	$\Delta\sigma$
24	111	-244.0	218.9	462.9	1.54E-03	2.14E-03	3.68E-03	175	-794.8	239.5	239.5	158	-920.2	192.7	1112.9
2018	80	-108.2	241.0	349.2	1.25E-03	1.59E-04	1.41E-03	8	-666.0	149.5	149.5	60	-694.2	139.9	834.1
4011	173	-192.4	213.4	405.8	2.95E-04	1.68E-03	1.97E-03	161	-653.7	-14.2		88	-1087.4	-193.0	894.4
5305	102	-90.0	229.4	319.4	6.50E-04	2.83E-04	9.33E-04	17	-616.4	-18.5		83	-1012.9	-167.4	845.5
23	34	19.8	205.2	185.4	1.88E-04	5.77E-05	2.46E-04	117	137.1	279.4	142.3	168	-203.5	153.8	357.3
4014	166	-14.0	207.3	221.3	1.41E-04	*6.70E-06*	1.48E-04	86	-463.5	57.6	57.6	92	-467.4	57.1	524.5
4015	4	-15.6	195.3	210.8	9.46E-05	5.64E-05	1.51E-04	122	-598.1	-23.0		139	-636.7	-25.4	611.3

The stress field generated within the whole analysed sector is generally tri-axial and non-proportional, particularly during the disk acceleration and deceleration. During both phases, the ratio of the principal stresses and the bi-axial ratio continuously change, the corresponding Mohr's circles of stresses and strains continuously alter their centres and sizes and the principal axes are continuously rotating. The present results may give an answer of the question relevant to the direction of the early fatigue crack growth (FCG) of the initiated

cracks. FCI and early stage I mode II FCG are both cyclic plastic shear processes [5]. Thus, it is expected to have them along the plane of maximum cyclic shear stress range, $\Delta\tau_{max}$. The plane of $\Delta\tau_{max}$ was identified within the seven probable FCI sites. Table 1 lists $\Delta\tau_{max}$ for the sites together with the corresponding angles and minimum and maximum values of τ. The different entrance angles to the surface for different contact sites are common experimental observations in FF tests throughout different contact geometries, e.g. [4, 5].

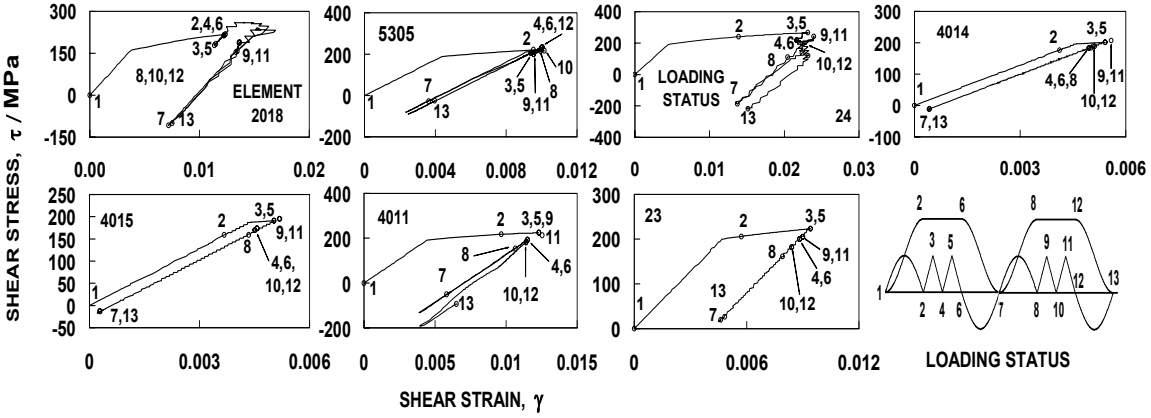

Fig. 4 variation of τ acting on the plane of $\Delta\tau_{max}$ plotted against the corresponding shear strain, γ, for the sites which experience cyclic plastic strain

The stress field generated within the whole analysed sector is generally tri-axial and non-proportional, particularly during the disk acceleration and deceleration. During both phases, the ratio of the principal stresses and the bi-axial ratio continuously change, the corresponding Mohr's circles of stresses and strains continuously alter their centres and sizes and the principal axes are continuously rotating. The present results may give an answer of the question relevant to the direction of the early fatigue growth of the initiated cracks. FCI and early stage I mode II FCG are both cyclic plastic shear processes [5]. Thus, it is expected to have them both along the plane of maximum cyclic shear stress range, $\Delta\tau_{max}$. The plane of $\Delta\tau_{max}$ was identified within the seven probable FCI sites. Table 1 lists $\Delta\tau_{max}$ for the sites together with the corresponding angles and minimum and maximum values of τ. The different entrance angles to the surface for different contact sites are common experimental observations in FF tests throughout different contact geometries, e.g. [4, 5]. Figure 4 shows, for the initiation sites, the variation of τ acting on the plane of $\Delta\tau_{max}$ plotted against the corresponding shear strain, γ. It is suggested to link the cyclic plastic shear strain range, $\Delta\gamma^p$, resulting from the second cycle with the duration of the initiation of stage I fatigue crack, N_i.

The possibility of developing an early stage I crack to a stage II crack can be addressed. Fatigue cracks are likely to develop in regions of tension. Thus, there are two possibilities for the growth development of initiated fatigue cracks. At some instance (i) an early stage I FCG may become non-propagating or (ii) a change from early stage I mode II FCG to a stage II mode I FCG may take place. The three disc elements 4011, 4015 and 5305 do not experience tensile principal stresses as a result of the applied loading and, thus, an initiated crack within those elements is expected to stop propagation. The initiated crack in the other four elements may develop and propagate through their material with a deviation in their crack paths. Mode I FCG is controlled by the maximum range of cyclic tensile stress, $\Delta\sigma_T$. In

Table 1, the plane of maximum $\Delta\sigma_T$ is identified for each initiation site together with the corresponding angles and minimum value of normal stresses. The results corresponding to the maximum cyclic normal stress are different.

Figure 5 presents the sites of the seven elements. The planes of $\Delta\tau_{max}$, label 1, represent the direction of early stage I cracks, see Table 1. The planes of $\Delta\sigma_{Tmax}$, label 2, represent the direction of the stage II cracks. The planes of $\Delta\tau_{max}$ within the elements 24, 2018 and 4014 have their shear stresses alternating in sign. This may result in FCG both deeply into the material and towards the surfaces. The latter development suggests a possible mechanism responsible for the formation of free relatively large material particles inside the mouth of fretting cracks, i.e. the shaded areas. Those particles have borders matching the borders of the corresponding crack mouth [1, 8 and 9].

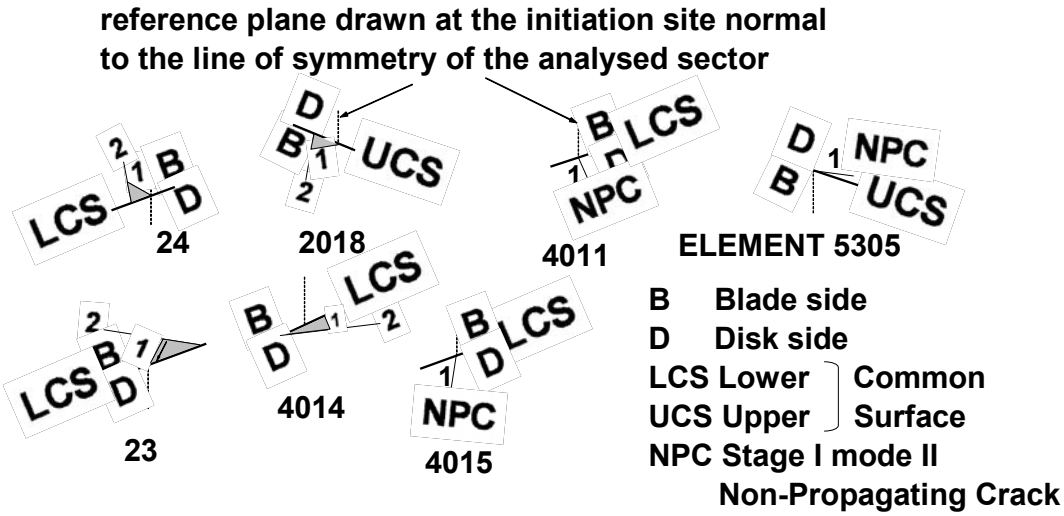

Fig. 5 possible cracking development of cracks initiated by FF

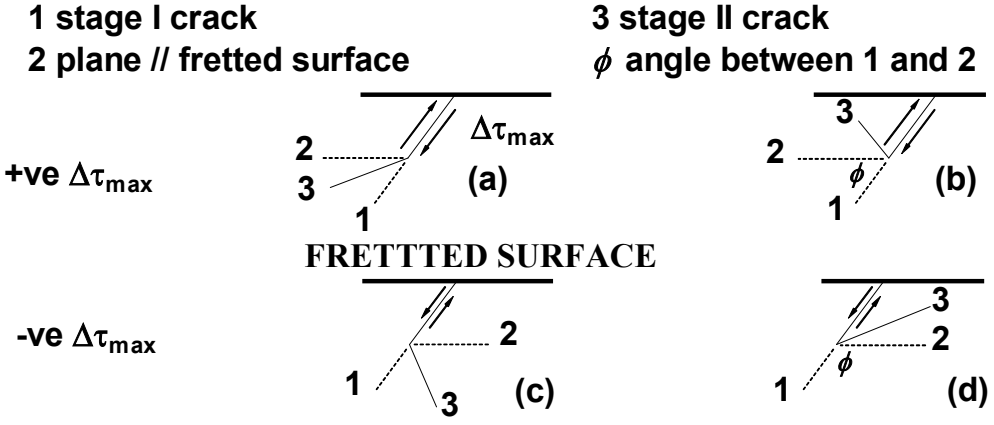

Fig. 6 Possible mechanism to form particles inside the mouth of FF cracks

The shear stress acting on the FCI plane is represented in Fig. 6 by two arrows. That plane divides the considered material into two parts. The inclination of the critical plane of $\Delta\sigma_{Tmax}$

predicts the probable development of that crack. When $\Delta\sigma_{Tmax}$ is sufficient to continue propagation, Fig. 6 shows different possibilities of that development. Two possibilities can result should $\Delta\tau_{max}$ be either negative or positive. Two dashed lines are plotted at the tip of the shear crack to represent (i) its continuation, i.e. plane 1, and (ii) a plane parallel to the fretted surface in the part which has the shear stress arrow directed towards the surface, i.e. plane 2. An angle, ϕ , is defined between the two planes. A kinked mode I crack is expected to propagate deeply into the material when the critical plane of $\Delta\sigma_{Tmax}$ deviates such that it is located within ϕ. Otherwise, the kinked crack is expected to grow towards the fretted surface to form free particles. The two types of crack propagation are, thus, expected when $\Delta\tau_{max}$ alternates in sign.

CONCLUSIONS

1. Along the contact surfaces of axial dovetail joints, multiple cracking sites with different crack entrance angles to the surface are probable near the dovetail notch base. However, the microstructure will have a strong influence on the crack initiation sites.
2. The free broken relatively large material particles experimentally found filling the mouth of FF cracks is possibly formed by surface cracking. The present model only predicts the cracking sites/development disregarding tribo-oxidation effects.

REFERENCES

1. Conner, B. P., Hutson, A. L., and Chambon, L. (2003) Wear **255**, 259–268
2. Nowell, D., and Hills, D. (1990) Wear **136**, 329–343
3. Shinde, S. and Hoeppner, D. W. (2005) Wear **259**, 271–276
4. Terheci, M., (2000) Materials Characterization **45**, 1-15
5. Proudhona, H., Fouvry, S. and Buffy, J. Y., (2005) Int. J. Fatigue **27**, 569–579
6. Fouvry, S., Kapsa, P., Sidoroff, F., and Vincent, L., (1998) J Phys IV **8**, 159–166
7. Ding, J., Leen, S. B. and McColl, I. R. (2004) Int. J. Fatigue, **26**, 521-531
8. Smith, K., Watson, P., and Topper, P., (1970) J Mater, **5**, 767–78
9. Golden, P. J., Bartha, B. B., Grandt, A. F. and Nicholas, T., (2004) Int. J. Fatigue **26**, 281-288
10. Meguid, S. A., (2000) Proc. Seventh Cairo University International MDP Conference, 161-172
11. Burguete, R. L. and Patterson, E. A., (2001) Proc. Institution of Mechanical Engineers, **215**, 113-123
12. Ruiz, C., and Nowell, D., (2000) In: Fracture mechanics, applications and challenges, 73–95, Fuentes, M., Elices, M., Martin-Meizoso, A., and Martinez-Esnaola, JM., (Ed.), ESIS publication **26**, Elsevier, Amsterdam
13. Hammouda, M. M. I., El-Batanony, I. G., and Sallam, H. E. M., (2003) Fat Fract Engng Mat Struct, **26**, 1-13
14. Morrissey, R. J., and Nicholas, T. (2005) Int. J. Fatigue, **27**, 1608-1612